Available online at www.sciencedirect.com
ScienceDirect
Biochimica et Biophysica Acta 1767 (2007) 1169–1179
Biochimica et Biophysica Acta BBA
www.elsevier.com/locate/bbabio

Thermodynamic and kinetic characterisation of individual haems in multicentre cytochromes c_3

Catarina M. Paquete [a], David L. Turner [a,b], Ricardo O. Louro [a], António V. Xavier [a,†], Teresa Catarino [a,c,*]

[a] *Instituto de Tecnologia Química e Biológica, Universidade Nova de Lisboa, Rua da Quinta Grande, 6, Apt. 127, 2780-156 Oeiras, Portugal*
[b] *School of Chemistry, University of Southampton, Southampton SO17 1BJ, UK*
[c] *Departamento de Química, Faculdade de Ciências e Tecnologia, Universidade Nova de Lisboa, Quinta da Torre, 2829-516 Caparica, Portugal*

Received 10 May 2007; accepted 25 June 2007
Available online 4 July 2007

Abstract

The characterisation of individual centres in multihaem proteins is difficult due to the similarities in the redox and spectroscopic properties of the centres. NMR has been used successfully to distinguish redox centres and allow the determination of the microscopic thermodynamic parameters in several multihaem cytochromes c_3 isolated from different sulphate-reducing bacteria. In this article we show that it is also possible to discriminate the kinetic properties of individual centres in multihaem proteins, if the complete microscopic thermodynamic characterisation is available and the system displays fast intramolecular equilibration in the time scale of the kinetic experiment. The deconvolution of the kinetic traces using a model of thermodynamic control provides a reference rate constant for each haem that does not depend on driving force and can be related to structural factors. The thermodynamic characterisation of three tetrahaem cytochromes and their kinetics of reduction by sodium dithionite are reported in this paper. Thermodynamic and kinetic data were fitted simultaneously to a model to obtain microscopic reduction potentials, haem–haem and haem–proton interacting potentials, and reference rate constants for the haems. The kinetic information obtained for these cytochromes and recently published data for other multihaem cytochromes is discussed with respect to the structural factors that determine the reference rates. The accessibility for the reducing agent seems to play an important role in controlling the kinetic rates, although is clearly not the only factor.

Keywords: Cytochrome c_3; Thermodynamic characterisation; Electron transfer kinetics; Multicentre protein; *Desulfovibrio*

1. Introduction

Sulphate-reducing bacteria are anaerobes with a highly versatile metabolism, having a large variety of electron transfer proteins. Tetrahaem type I cytochrome c_3 (TpIc_3) is a periplasmic protein found in all organisms belonging to the *Desulfovibrionaceae* family, where it is produced in large quantities [1]. It is a small (13.5–15 kDa) soluble protein that contains four *c*-type haems, covalently bound to the polypeptide chain through thioether bonds, with bis-histidinyl axial coordination. TpIc_3 is considered to be the physiological partner of the periplasmic hydrogenase and is an essential component of the electron transport chain, coupling the oxidation of molecular hydrogen to sulphate respiration that occurs in the cytoplasm [2,3].

Structures of cytochromes c_3 isolated from various sulphate-reducing bacteria species have been determined by X-ray crystallography [4–10] and by Nuclear Magnetic Resonance (NMR) [11–13]. The architecture of the haem core is conserved in these cytochromes despite the lack of homology in their aminoacid sequence, and is also observed in other membrane-associated cytochromes such as type II cytochrome c_3 (TpIIc_3) [7]. Due to their close proximity, the haems present homotropic

Abbreviations: TpIc_3, Type I cytochrome c_3; TpIIc_3, Type II cytochrome c_3; *D.*, *Desulfovibrio*; *Dsm.*, *Desulfomicrobium*; NMR, Nuclear Magnetic Resonance

* Corresponding author. Instituto de Tecnologia Química e Biológica, Universidade Nova de Lisboa, Rua da Quinta Grande, 6, Apt. 127, 2780-156 Oeiras, Portugal. Fax: +351 21 4428766.
E-mail address: catarino@itqb.unl.pt (T. Catarino).
† Deceased 7th May 2006.

0005-2728/$ - see front matter © 2007 Elsevier B.V. All rights reserved.
doi:10.1016/j.bbabio.2007.06.005

redox cooperativity [14]. Furthermore, the reduction potential of the haems is very negative and pH dependent in the physiological pH range (redox–Bohr effect). These properties allow TpIc_3 to receive the electrons and protons produced by hydrogenase in the oxidation of molecular hydrogen and perform energy transduction, activating protons which can drive ATP synthesis [2].

Apart from NMR several techniques have been used to study the electron transfer process in these proteins including Mossbauer spectroscopy [15], electron paramagnetic resonance (EPR) [16–20], cyclic voltammetry [21,22], pulse radiolysis [23] and resonance Raman [24]. Discrimination of the midpoint reduction potentials of the haems is usually difficult because of their close proximity and the potentials obtained are generally macroscopic, since interactions among the haems cannot be considered. These methods also lack information to attribute redox potentials to specific haems in the structure.

NMR spectroscopy however, can be used to follow individual haems in the structure of multihaem proteins, particularly through the resonances of methyl substituents. The four haem irons in cytochromes c_3 are low spin, and the methyl resonances are usually well resolved in the paramagnetic ($S=1/2$) oxidised form. Dobson et al. [25] and McDonald et al. [26] used NMR to study the intermediate oxidation stages which develop between the fully reduced and the fully oxidised states of cytochrome c_3 from *Desulfovibrio vulgaris* Hildenborough and *Desulfovibrio gigas*. However, due to difficulties in achieving full reduction and to poor sensitivity, these early reports are incomplete. Moura et al. [27] analysed the complete NMR reoxidation pattern of *D. vulgaris* Hildenborough cytochrome c_3 taking into account the 16 redox microstates that correspond to different configurations of oxidised and reduced haems in the four-centre molecule.

In 1984, Santos et al. [14] used NMR data to calculate nine thermodynamic parameters for *D. gigas* cytochrome c_3: three relative reduction potentials and six haem–haem interacting potentials for each pH value studied. However, the absolute values for the reduction potentials were not measured and the interactions appeared to be pH dependent, although with large uncertainties. Coletta et al. [28] therefore proposed a thermodynamic model with distinct acidic and basic forms and sought to determine its parameters from the same NMR data set and potentiometric titrations followed by visible spectroscopy, but the 21 parameters (four haem reduction potentials and six haem–haem redox interaction potentials for each form plus one pK_a) are ill-defined. In fact there is no evidence for a major conformational change between acidic and basic forms and the pH dependence can be explained by interactions between the ionisable group and each of the four haems [29]. This leads to a model that involves five charged centres (four haems with their reduction potentials and one acid–base centre with its pK_a) and pairwise interactions between them (six haem–haem interactions and four redox–Bohr interactions), reducing the number of parameters to 15. This model, and its extension to include two ionisable centres, has been used for the detailed characterisation of several tetrahaem cytochromes c_3 [9,29–32] and also a trihaem cytochrome c_3 [33].

Kinetic data on the electron transfer between small artificial electron donors and cytochrome c_3 has also been obtained using several techniques [9,23,32–42]. In some of these studies the kinetic traces are treated as sums of exponentials [34,37]; the rate constants obtained would be those of individual haems only if there is no haem–haem interaction and no intramolecular electron transfer, otherwise there is no simple relationship. In fact, electron transfer within cytochromes c_3 tends to be extremely fast and so the process of reduction (or oxidation) of each molecule is properly described as a series of one-electron steps [35]. The rate constants for the consecutive steps are measurable, particularly with the use of samples that are partially reduced [39,40,42], but the rates only correspond to the reduction rates of individual haems if the redox potentials are widely separated and the rates follow the order of reduction, such that the first haem to be reduced is also the fastest, and so on. Catarino et al. [39] used a thermodynamic approach to deconvolute the rate constants for the reduction of the individual haems of *D. gigas* cytochrome c_3, again assuming different properties for acidic and basic forms of the protein. It is clear that it is not generally possible to separate the contributions of different centres to the kinetic traces without having a complete thermodynamic characterisation, which was not available at the time. The thermodynamic model of pairwise interactions [29] is sufficiently simple for all of the parameters to be determined, and it provides the necessary basis for analysing kinetic properties. Catarino and Turner [41] used the thermodynamic parameters to determine the concentrations of all of the redox microstates in the protonated and deprotonated forms and used Marcus theory [43] to determine the contribution of the driving force to the rate of reduction of each haem in each one-electron step (there are 64 such steps in the presence of one acid/base group). The remaining factor in the individual rates is a reference rate constant that reflects the different environment of each haem. Since each kinetic trace provides a maximum of four parameters, it is assumed that each haem has a different reference rate constant that remains constant throughout the reduction and is not changed by protonation. This model has been used to characterise the kinetic behaviour, including its pH dependence, of several tetrahaem cytochromes c_3 [9,32], and of a trihaem cytochrome c_3 [33].

In this work an extensive set of data obtained for different cytochromes c_3 is fitted simultaneously to the thermodynamic and kinetic models as a rigorous test of their applicability, and the resulting kinetic parameters are discussed with respect to the protein structures.

2. Materials and methods

2.1. Thermodynamic studies

2.1.1. Sample preparation

The NMR samples of cytochrome c_3 from and *D. gigas* and *D. vulgaris* Hildenborough were prepared in the reduced and intermediate stages of oxidation at different pH values as previously described [29]. The ionic strength was adjusted to 50 mM by addition of KCl.

2.1.2. NMR spectroscopy

Two-dimensional 1H-NMR spectra were collected in a Bruker DRX-500 spectrometer at 298.0±1.0 K. The NMR data were obtained as previously described [44].

2.1.3. Visible spectroscopy

Anaerobic redox titrations of the cytochromes c_3 followed by visible spectroscopy were performed at 298.0±1.0 K as described in the literature [9]. *D. gigas* and *D. vulgaris* Hildenborough cytochrome c_3 solutions were prepared in 50 mM Tris/maleate buffer at pH 6.5 and 7.8, and *Desulfovibrio desulfuricans* ATCC 27774 cytochrome c_3 solutions were prepared in 100 mM Tris/maleate buffer at pH 6.4 and 7.9. All buffers and protein solutions were prepared inside an anaerobic chamber. To ensure rapid equilibration between the electrode and the redox centres of the protein a mixture of redox mediators was selected according to the procedures defined in the literature [45]: methyl viologen, neutral red, diquat, safranine O, anthraquinone 2,7-disulfonate, anthraquinone 2-sulfonate, indigo tetrasulfonate, indigo disulfonate and indigo trisulfonate were used for all experiments. To this mixture were added phenosafranine for the titrations performed at pH 6, and methylene blue and gallocyanine for the ones performed at pH 7. Different concentration ratios of protein *versus* mediators were tested in order to check for possible effects resulting from specific interaction of mediator molecules with the protein. For each protein and pH value the redox titrations were repeated at least twice, both in the oxidative and reductive directions to check for hysteresis and reproducibility.

The reduced fraction of the cytochrome c_3 was determined by integrating the area of the α peak above the line connecting the flanking isosbestic points in order to subtract the optical contribution of the redox mediators. The data presented here were obtained with protein concentrations of ca. 40 μM and 1.2–2 μM for each mediator.

2.2. Kinetic studies

2.2.1. Sample preparation

Stock solutions of cytochromes c_3 from *D. vulgaris* Hildenborough, *D. gigas* and *D. desulfuricans* ATCC 27774 were degassed with cycles of vacuum and argon in order to remove dissolved oxygen and transported into an anaerobic chamber. The buffer solutions were prepared inside the anaerobic chamber with degassed water. Tris/maleate buffer in the pH range 5.5–8.5 was used in all kinetic experiments and the actual pH of the reaction was measured after each experiment. The concentration of the buffers after mixing was 50 mM for *D. vulgaris* Hildenborough and *D. gigas* cytochromes c_3, and 100 mM for *D. desulfuricans* ATCC 27774 cytochrome c_3. The concentration of protein was determined after each experiment by UV-visible spectroscopy using ε_{552}= 120 000 M^{-1} cm^{-1} for the reduced protein. The concentration of the protein was 1–2 μM after mixing.

The reducing agent, sodium dithionite, was recrystallised to give > 95% pure material. The recrystallisation of commercial sodium dithionite was based on the work of C. McKenna [46] adapted to be performed inside an anaerobic chamber. Solid sodium dithionite was added to degassed Tris/maleate buffer 5 mM at pH 8.5, inside the anaerobic chamber, to give the approximate desired concentration. The ionic strength of this buffer was set to 100 mM with KCl, for the experiments with *D. desulfuricans* ATCC 27774 cytochrome c_3. For each experiment the actual concentration of the reducing agent was measured, inside an anaerobic chamber, by UV-visible spectroscopy using ε_{314}=8 000 M^{-1} cm^{-1} [47]. The concentration of sodium dithionite was 100–200 μM after mixing. The nature of the reducing species was determined according to the method of Lambeth and Palmer [48].

2.2.2. Data collection

Rapid mixing kinetic experiments were carried out on a HI-TECH Scientific SF-61 stopped-flow instrument inside an anaerobic chamber where the oxygen level was kept below 0.2 ppm. The data were acquired at 552 nm using a large excess of dithionite to guarantee irreversible pseudo first order kinetics in practice. The temperature was kept at 298.0±1.0 K using an external circulating bath.

The reference value for the optical density (OD) of the protein in the fully oxidised state was obtained by mixing the protein with potassium ferricyanide, and the reference value for the OD in the fully reduced state was obtained from the final absorbance taken at effectively infinite time after each experiment.

To perform rapid mixing kinetics with various degrees of reduction of the starting material a few microliters of a concentrated sodium dithionite solution was added to the protein solution before the experiment to give the desired degree of reduction.

The experimental data obtained for the different cytochromes c_3 at different pH values was normalised in order to have oxidised fraction *versus* time. The time scale was corrected for the dead time of the apparatus.

2.2.3. Thermodynamic and kinetic modelling

The data from redox titrations followed by NMR and by visible spectroscopy and from kinetic experiments were fitted simultaneously to a thermodynamic model [29] and to a kinetic model [41]. These models consider 5 or 6 [31] charged centres interacting with each other, which correspond to the four haems and one or two acid base groups.

Working in conditions of fast intramolecular electron exchange and slow intermolecular electron exchange in the NMR timescale, a separate set of NMR resonances is observed for the protons of the haems in each of the five oxidation stages (numbered 0–4, according to the number of oxidised haems). The resonance positions and line widths of one methyl group from each haem can be followed in different stages of oxidation, at different pH values. These chemical shifts depend on the ratio between the molar fraction of the microstates in which the haem considered is oxidised and the states in which the same haem is reduced. Thus the shifts are governed by the relative microscopic redox potentials of the haems in that stage of oxidation. The choice of the methyl group to be followed is important and it should preferably point towards the protein surface to minimise the contribution from the extrinsic dipolar shifts caused by nearby oxidised haems. Nevertheless, the chemical shifts were corrected for these extrinsic paramagnetic shifts using methods described in the literature [49].

The observation of intermediate stages of oxidation in the NMR data only establishes the relative reduction potentials of the haems. The calibration of the absolute potentials and of the haem–haem interactions was done using data from redox titrations followed by visible spectroscopy.

The complete kinetic scheme for electron transfer between a four centre protein and a one-electron donor is extremely complex and intractable. Even with the simple collisional approach and no pH dependence, 16 microstates with 32 possible electron transfer microsteps must be considered. However if the electron transfer between protein molecules is slow and the intramolecular electron transfer between the centres is fast on the time scale of the experiment, this complex system collapses into a simple kinetic scheme of 4 consecutive macroscopic electron transfer steps and so it yields only 4 measurable rate constants [41]. Under these conditions the distribution of electrons inside the multicentre protein is thermodynamically controlled within each redox stage, and the rate constant of each step is a population weighted average of the rate constants of the microscopic electron transfer steps that contribute to that particular step. The relation between rates of different microsteps where the same haem is being reduced can be obtained using Marcus theory for electron transfer [43] and a set of reasonable assumptions [41]. The rate constants of the microsteps depend on the thermodynamic driving force, on the reorganisation energy (λ) and on structural factors that account for distance, orientation and binding affinity between the electron donor and the protein. Assuming that the reorganisation energy and the structural factors do not change during the reduction process, the rate constant of a particular microstep, k_i^j (i is the centre that is being reduced in microstep j), can be expressed as a reference rate constant, k_i^0, multiplied by an exponential factor that accounts for the driving force associated with electron transfer in that microstep (Eq. (1)):

$$k_i^j = k_i^o \exp\left[\frac{e_i^j F}{2RT}\left(1 + \frac{e_D F}{\lambda} - \frac{e_i^j F}{2\lambda}\right)\right] \quad (1)$$

In Eq. (1) e_i^j is the microscopic midpoint potential of centre i when it is reduced in microstep j, e_D is the midpoint potential of the electron donor (−0.3 V) [50], and λ is the reorganisation energy, taken as 1 eV [51]. In model 1 [41] the values of e_D and λ are assumed to be constant during the reduction process and each centre is assigned a reference rate constant, making up the 4 variables available to describe the system.

According to this model, the shape of the kinetic curves also contains information about the midpoint potentials of the redox centres, their pH dependence, and the interactions between them. Therefore, the NMR, visible, and kinetic data were fitted simultaneously, using the Marquardt method, to obtain the thermodynamic parameters and the reference rate constants of the centres.

3. Results

Two-dimensional exchange-correlated NMR spectra of cytochromes c_3 from *D. vulgaris* Hildenborough and *D. gigas* were obtained under conditions (ionic strength and temperature) of fast intramolecular electron exchange and slow intermolecular electron exchange in the time scale of the experiments. The chemical shift and the line width of one methyl group resonance from each haem were measured in each stage of oxidation at different pH values. New NMR experiments for *D. vulgaris* Hildenborough and *D. gigas* cytochromes c_3 were performed at a higher ionic strength than those published previously [29,30] to match the experimental conditions used in the visible redox titrations and kinetic experiments. Since the results showed that the increase in ionic strength had no significant effect on the chemical shifts of the methyl groups, old

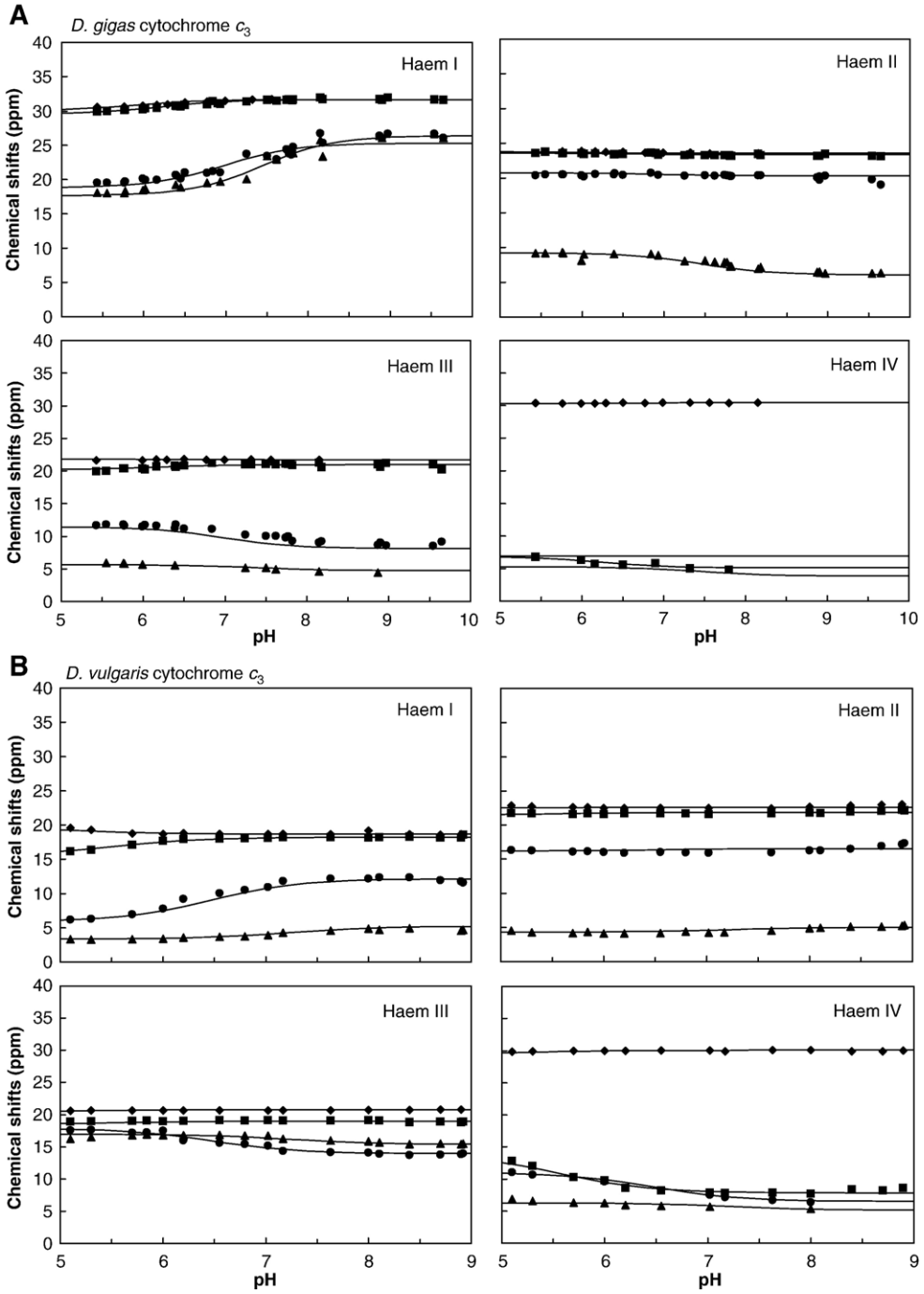

Fig. 1. pH dependence of the ^{1}H-NMR chemical shifts of one methyl group from each of the four haems in different stages of oxidation (stages 1 (△), 2 (○), 3 (□) and 4 (◇)): (A) *D. gigas* cytochrome c_3 with M18^1 I, M7^1 II, M12^1 III and M18^1 IV; (B) *D. vulgaris* Hildenborough cytochrome c_3 with M2^1 I, M18^1 II, M12^1 III and M18^1 IV; (C) *D. desulfuricans* ATCC 27774 cytochrome c_3 with M18^1 I, M18^1 II, M12^1 III and M18^1 IV. The full lines represent the best fit of the data using the parameters reported in Table 1.

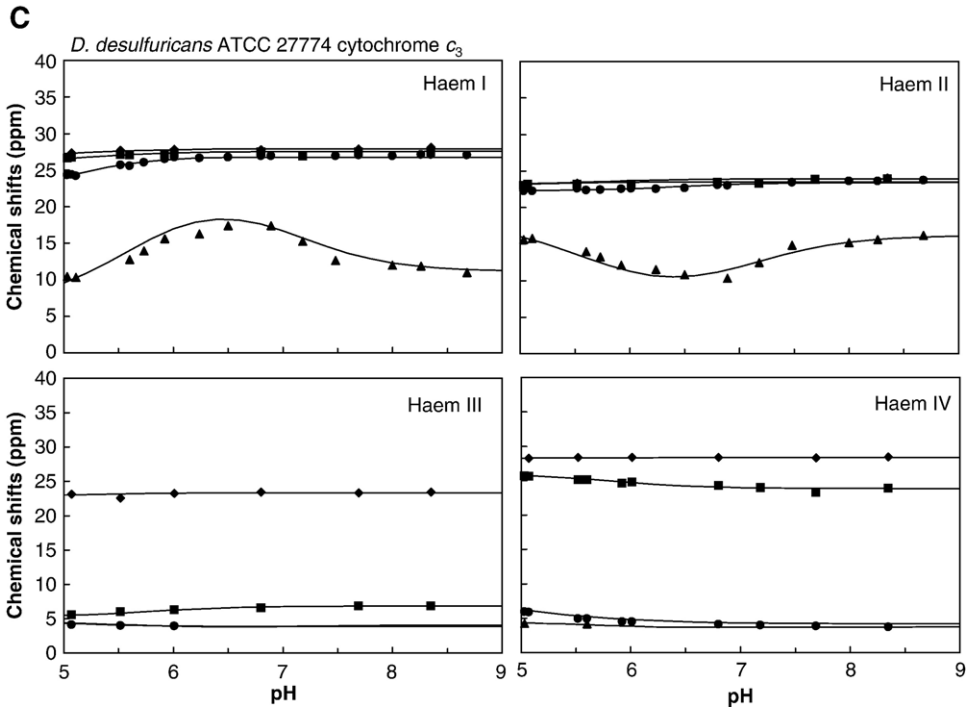

Fig. 1 (*continued*).

and new NMR data were used together in the fittings (Fig. 1). The NMR data used for the characterisation of *D. desulfuricans* ATCC 27774 cytochrome c_3 were those previously published [31] (Fig. 1).

The redox titrations followed by visible spectroscopy allow the calibration of the relative values of redox potentials and interactions to the absolute redox scale. The data used for the fittings (Fig. 2) are fully reversible, reproducible, and free of distortions caused by interaction with the redox mediators since it did not change with further decreasing the ratio of mediators *versus* protein.

The kinetic data for the fully oxidised samples are shown in Fig. 3. The traces are typically biphasic, which indicates that the rates of only two out of the four possible electron transfer steps can be measured from a single trace. However, this information is supplemented by experiments with partially reduced starting materials (data not shown) and, most importantly, the traces are pH dependent.

The observed rate constants obtained from exponential fittings of kinetic traces acquired at a single pH for different sodium dithionite concentrations show a linear dependence on the square root of the dithionite concentration for the three cytochromes [34, 39 and this work (data not shown),] indicating that the reducing species is $SO_2^{\bullet-}$, the dissociation product of dithionite. Therefore, the rate constants are calculated with respect to the concentration of $SO_2^{\bullet-}$ using the dissociation constant given by Lambeth and Palmer, $K_d = 1.4 \times 10^{-9}$ M [48].

The curves obtained from the simultaneous fit of the thermodynamic and kinetic models to the full set of NMR, visible redox titration, and kinetic data are presented in Figs. 1–3. Table 1 reports the optimised thermodynamic parameters obtained for each protein where the diagonal terms are the free energies of oxidation (haems I to IV) and deprotonation of the acid–base centre in the fully reduced and protonated form. Above the diagonal are the pairwise coupling energies between the redox centres, and between the redox centres and the acid–base centre(s). Table 2 presents the macroscopic pK_as for the ionisable(s) centre(s) associated with each of the five stages of oxidation for the different cytochromes c_3.

Due to the pH dependence of the NMR data for *D. desulfuricans* ATCC 27774 cytochrome c_3 it was necessary to add one extra acid–base centre to the 5-centre thermodynamic model [31]. However due to the lack of features in the NMR spectroscopic data it was not possible to define the interactions between this extra acid–base centre and the haems II, III and IV, the interaction of the first acid–base centre with haem I, or the proton–proton interaction.

All the haems in the cytochromes studied in this work show negative energies of interaction with the acid–base centre, i.e. positive heterocooperativity, as expected on electrostatic grounds for transfer of particles with opposite charges. The reduction potential of haem I is always one of the most affected by pH, which is in agreement with the identification of propionate 13 of haem I (nomenclature according to the IUPAC–IUB recommendations [52]) as the main residue responsible for the redox–Bohr effect in these cytochromes [30,31,53]. The haem–haem redox interaction energies should be positive, corresponding to negative homocooperativities, if they were caused solely by electrostatic effects. However, *D. gigas* and *D. vulgaris* Hildenborough cytochromes c_3 present negative redox interaction energies between some of the haems, which implies the existence of redox-related conformational changes such as those observed by NMR and X-ray studies [7,8,11,12,54]. These homotropic and heterotropic cooperativ-

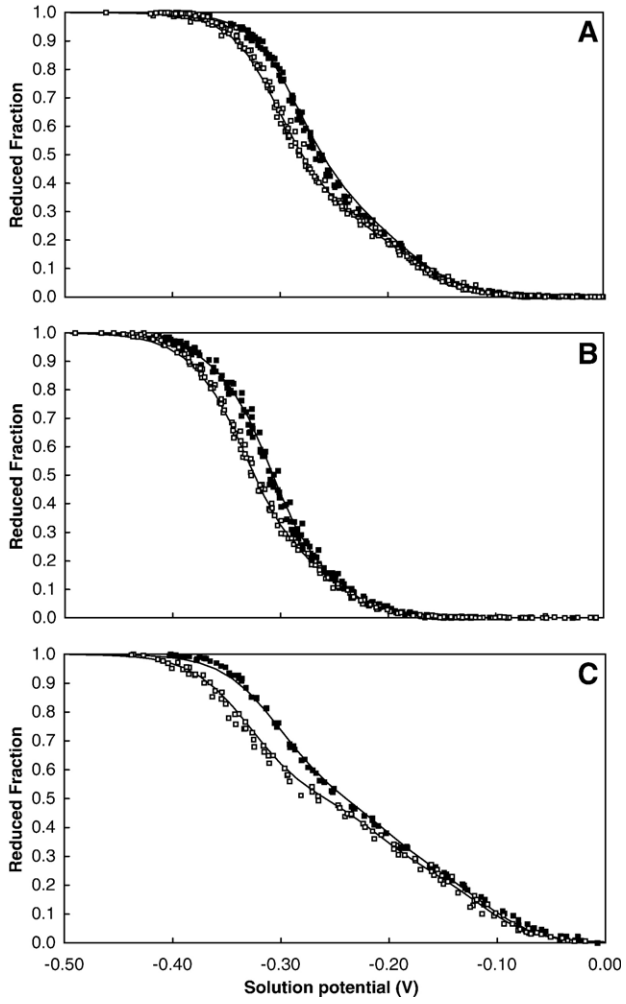

Fig. 2. Visible redox titrations performed at 298 K at different pH values: (A) *D. gigas* cytochrome c_3 at pH 6.5 (filled symbols) and pH 7.8 (open symbols); (B) *D. vulgaris* Hildenborough cytochrome c_3 at pH 6.5 (filled symbols) and 7.8 (open symbols); (C) *D. desulfuricans* ATCC 27774 cytochrome c_3 at pH 6.4 (filled symbols) and pH 7.9 (open symbols). The solid lines represent the best fit of the experimental data using the parameters reported in Table 1.

ities allow cytochrome c_3 to couple the transfer of electrons and protons, a process termed "proton-thrusting" [2], which is fundamental for its physiological function as partner of the periplasmic hydrogenase.

Fitting the kinetic traces of each cytochrome with the thermodynamic parameters previously determined [8,29,30] quantitatively reproduces their pH dependence. However, since the kinetic data cover a wider range of pH values than the redox titrations used to obtain the thermodynamic parameters, a small improvement is obtained by fitting the NMR, kinetic, and new visible titration data simultaneously for each cytochrome. This did not change any of the thermodynamic parameters significantly. The fitted kinetic curves are presented in Fig. 3 and the reference rate constants for the individual haems, k_i^0, that were obtained in the fit are presented in Table 3, together with results from earlier studies [9,32].

In order to test the significance of the parameters obtained, we also applied model 2 of Catarino and Turner [41] (data not shown) in which it is assumed that the structural effects are identical for each haem in each oxidation stage but that they change as the protein is reduced. There are in fact conformational differences between fully oxidised and fully reduced cytochromes c_3 but they are small with respect to the differences between the environments of the four haems. This model is equivalent to model 1 only in the limit that the redox potentials of the haems are sufficiently well separated for one haem to be fully reduced in each reduction step, which is not the case in the cytochromes c_3 and so model 2 serves as an effective control.

The quality of the fit to model 1 was markedly better than that obtained with model 2 for *D. gigas*, *D. africanus* TpIc_3, and *D. africanus* TpIIc_3 and there was essentially no difference between the two models for *D. vulgaris* Hildenborough, *Dsm. norvegicum*, *Dsm. baculatum* and *D. desulfuricans* ATCC 27774. *Dsm. norvegicum* and *Dsm. baculatum* are closely similar proteins in all respects, and *D. desulfuricans* ATCC

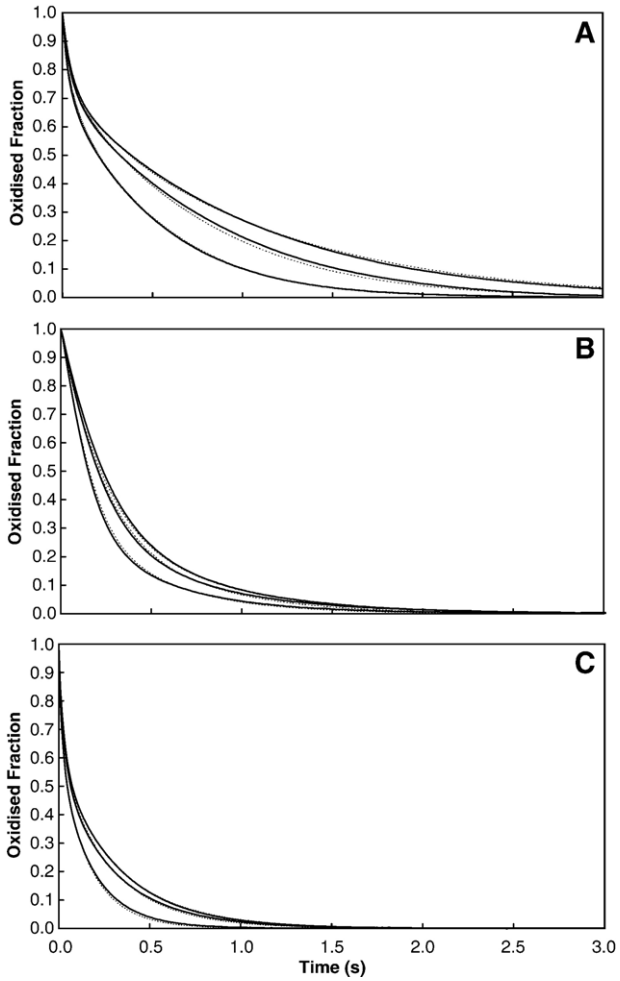

Fig. 3. Kinetics of reduction of various cytochromes c_3 by sodium dithionite at different pH values: (A) *D. gigas* cytochrome c_3 at pH 8.5 (upper trace), pH 7.3 (middle) and pH 6.1 (lower). The concentration of sodium dithionite was 109 μM and the concentration of protein was 1.3 μM; (B) *D. vulgaris* cytochrome c_3 at pH 8.5 (upper trace), pH 7.3 (middle) and pH 6.0 (lower). The concentration of sodium dithionite was 100 μM and the concentration of protein was 1.6 μM; (C) *D. desulfuricans* ATCC 27774 cytochrome c_3 at pH 8.4 (upper trace), pH 7.2 (middle) and pH 5.9 (lower). The concentration of sodium dithionite was 208 μM and the concentration of protein was 2.0 μM. The dotted curves are the fit to the data using the parameters reported in Tables 1 and 2.

Table 1
Thermodynamic parameters determined by fitting the NMR, visible and kinetic data for the *D. gigas*, *D. vulgaris* Hildenborough and *D. desulfuricans* ATCC 27774 cytochromes c_3

	Haem I	Haem II	Haem III	Haem IV	Ionisable centre
(A) D. gigas cytochrome c_3					
Haem I	**−279** (2)	−15 (3)	51 (3)	−16 (7)	−62 (2)
Haem II		**−262** (2)	−52 (4)	59 (4)	−25 (2)
Haem III			**−240** (3)	22 (3)	−38 (2)
Haem IV				**−227** (7)	−18 (3)
Ionisable centre					**491** (4)
(B) D. vulgaris cytochrome c_3					
Haem I	**−252** (2)	−39 (1)	19 (1)	3 (3)	−74 (3)
Haem II		**−284** (2)	1 (1)	10 (2)	−36 (2)
Haem III			**−343** (1)	34 (2)	−23 (2)
Haem IV				**−293** (2)	−14 (2)
Ionisable centre					**454** (3)

	Haem I	Haem II	Haem III	Haem IV	Ionisable centre H_1	Ionisable centre H_2
(C) D. desulfuricans ATCC 27774 cytochrome c_3						
Haem I	**−237** (2)	3 (2)	62 (6)	20 (5)	–	−88 (5)
Haem II		**−279** (2)	40 (10)	12 (6)	−63 (3)	–
Haem III			**−215** (9)	48 (2)	−55 (6)	–
Haem IV				**−206** (6)	−33 (4)	–
Ionisable centre H_1					**440** (3)	–
Ionisable centre H_2						**377** (4)

The fully reduced and protonated protein was taken as the reference state for all haems. Diagonal terms (in bold) are oxidation energies of the haems and deprotonation energies of the acid/base centre(s). Off-diagonals terms are the redox and redox–Bohr interactions energies. All values are reported in meV. Standard errors are given in parenthesis.

27774 is unusual insofar as two redox–Bohr interactions are required to explain the data but some of the additional parameters could not be defined. Since the trend of distinction between models 1 and 2 correlates well with the standard errors found for the reference rates of individual haems (Table 3), with the sole exception of *D. vulgaris* Hildenborough, it appears that the reduction rates of the individual haems are indeed measurable and distinguishable even though the uncertainties are quite large in some cases.

The complicated relationship between the rates of reduction of individual haems and the rates of the consecutive one-electron reduction steps is illustrated by considering the fraction of electrons entering the molecule through each haem in each step (Table 4), which can be calculated using the reference rate constants, the driving force for each microstep, and the populations of the microstates.

The first step of reduction In *D. gigas* cytochrome c_3 is dominated by haem IV, which has both the highest reference rate constant and the larger driving force (highest reduction potential). Since it is the first haem to be reduced, haem IV is less available in the subsequent steps of reduction because only a small fraction remains oxidised and ready to receive electrons (Fig. 4A).

Although haem IV is also the first to be reduced in *D. vulgaris* Hildenborough cytochrome c_3, haem II, which has the highest reference rate constant, also makes a significant contribution to the first reduction step (Fig. 4B). Haem III is reduced mainly in the last step but its direct reduction is slow

Table 2
Macroscopic pK_as for the ionisable(s) centre(s) associated with each of the five stages of oxidation for the *D. gigas*, *D. vulgaris* Hildenborough and *D. desulfuricans* ATCC 27774 cytochromes c_3

Cytochrome c_3	Stage 0	Stage 1	Stage 2	Stage 3	Stage 4
D. gigas	8.3	7.4	7.0	6.2	5.9
D. vulgaris	7.7	7.2	6.5	5.6	5.2
D. desulfuricans ATCC 27774	7.4	7.0	6.4	5.8	4.9
	6.4	6.2	5.3	5.0	4.9

Table 3
Reference rate constants for each haem, k_i^0, for all the cytochromes c_3 studied so far

$k_i^0/10^8$ M^{-1} s^{-1}	Haem I	Haem II	Haem III	Haem IV	Reference
D. gigas	7.0 (0.4)	0.0 (0.3)	3.9 (0.5)	10.0 (0.4)	This work
D. vulgaris Hildenborough	15.4 (0.6)	62.9 (0.8)	0.8 (0.8)	11.2 (0.8)	This work
D. desulfuricans ATCC 27774	13.9 (5.1)	14.7 (4.9)	2.0 (3.0)	9.6 (3.1)	This work
Dsm. norvegicum	5.0 (11.0)	97.0 (7.0)	5.1 (0.8)	1.0 (10.0)	[9]
Dsm. baculatum	16.0 (9.0)	98.0 (10.0)	3.4 (0.6)	0.0 (6.0)	[9]
D. africanus	8.2 (4.0)	16.5 (1.1)	1.2 (0.2)	6.4 (4.0)	[32]
D. africanus TpIIc_3	8.1 (0.9)	2.9 (2.7)	0.3 (4.9)	45.9 (4.0)	[32]

Standard errors calculated assuming an experimental error of 5% in the kinetic traces are given in parentheses.

Table 4
Fraction of electrons that enter the molecule through each haem in each one electron reduction step (step 1 is the first step of reduction, i.e. the protein receives one electron) for *D. gigas*, *D. vulgaris* Hildenborough, and *D. desulfuricans* ATCC 27774 cytochromes c_3 at pH 6.5

Cytochrome c_3	Step	Haem I	Haem II	Haem III	Haem IV	Sum/step
D. gigas	1	0.059	0.001	0.093	0.848	1.0
	2	0.428	0.002	0.307	0.263	1.0
	3	0.408	0.006	0.204	0.382	1.0
	4	0.577	0.004	0.142	0.278	1.0
	Sum/haem	1.47	0.01	0.75	1.77	
D. vulgaris Hildenborough	1	0.130	0.438	0.011	0.421	1.0
	2	0.211	0.683	0.009	0.097	1.0
	3	0.113	0.799	0.005	0.082	1.0
	4	0.105	0.721	0.027	0.147	1.0
	Sum/haem	0.56	2.64	0.05	0.75	
D. desulfuricans ATCC 27774	1	0.193	0.082	0.208	0.517	1.0
	2	0.202	0.152	0.050	0.597	1.0
	3	0.371	0.524	0.014	0.090	1.0
	4	0.508	0.423	0.015	0.055	1.0
	Sum/haem	1.27	1.18	0.29	1.26	

The values were calculated using the thermodynamic parameters presented in Table 1 and the microscopic rate constants calculated for the individual microsteps using the reference rate constants presented in Table 3.

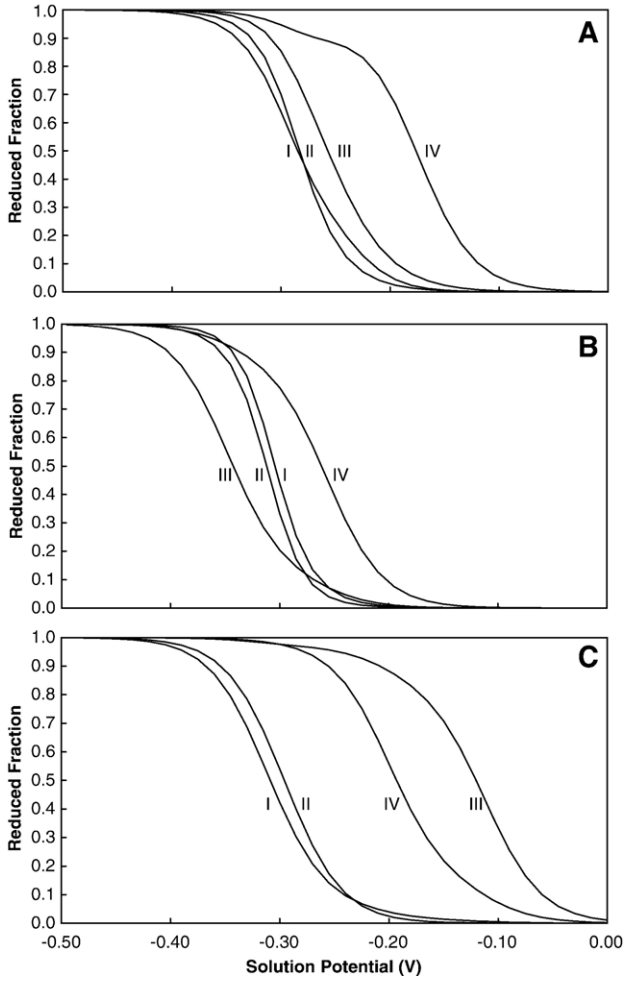

Fig. 4. Redox titration curves of individual haems for *D. gigas* (A), *D. vulgaris* Hildenborough (B) and *D. desulfuricans* ATCC 27774 (C) cytochromes c_3. The curves were calculated at pH 6.5 using the thermodynamic parameters presented in Table 1. The haems are identified by Roman numbers.

and so it is reduced by intramolecular electron exchange primarily through the small remaining oxidised population of haem II.

By contrast, haem III is the first to be reduced in cytochrome c_3 from *D. desulfuricans* ATCC 27774 and has the largest driving force, but it has the smallest reference rate constant and again it is reduced largely by intramolecular electron exchange (Fig. 4C).

4. Discussion

The characterisation of individual centres in multicentre proteins is challenging but essential to understanding their function. The tetrahaem cytochromes c_3 are particularly difficult to study because NMR is the only technique that can distinguish the haems clearly under physiological conditions, and yet we have shown that it is possible to use a combination of NMR and redox titrations to measure the microscopic reduction potentials and interactions of the haems [9,29–33]. In this work, we have collected new thermodynamic and kinetic data for three cytochromes c_3 which, together with recently published data for four others, provides an opportunity to examine the possibilities for extracting kinetic information for individual centres.

In principle, the rate of reduction of each haem by $SO_2^{\bullet-}$ could depend on the redox state of the other haems, giving 32 distinct one-electron steps, as well as on the protonation state of a redox–Bohr group which increases the number to 64. However, internal equilibration of individual molecules between electron transfer steps means that each kinetic trace provides at most four parameters, and they are typically only mono- or bi-exponential in practice [41]. Although the measurements can be extended by varying pH and partially reduced initial states, it is clearly not possible to treat all of the microsteps independently. The problem is simplified by using Marcus theory [43] together with the thermodynamic parameters to separate the effect of the driving force for each microstep from factors such as the distance from the $SO_2^{\bullet-}$ to the haem at the point of electron transfer. This shifts the focus to the local structure around the haems and we can define one reference rate for each haem that combines all of the non-thermodynamic factors. In this model, referred to as model 1 [41], only four parameters are required and it becomes possible to determine them experimentally.

Despite the similarities in the protein folds and haem architecture, there are dramatic differences in the reference rates of reduction obtained for the different haems (Table 3) and also for the relative rates of the haems within each cytochrome. Haems I and IV have intermediate rates (ca. 10^9 M^{-1} s^{-1}) in all cases except for *D. africanus* TpIIc_3, which is the only example

Table 5
Global and weighted accessibility for the reducing agent to the haems for *D. gigas*, *D. vulgaris*, *D. desulfuricans* ATCC 27774, *D. africanus*, *Dsm. norvegicum*, *Dsm. baculatum* TpI cytochromes c_3 and *D. africanus* TpII cytochrome c_3 (global and weighted values calculated from the X-ray structures [4–10] with a sphere of radius 2.5 Å (see text)); and solvent exposure calculated for a water molecule with a sphere of radius 1.4 Å

Cytochrome c_3	Accessibility		Haem I	Haem II	Haem III	Haem IV
D. gigas	$SO_2^{\bullet-}$	global	167	194	145	91
		weighted	2.31	4.41	2.82	7.88
	H_2O	global	254	238	228	118
D. vulgaris Hildenborough	$SO_2^{\bullet-}$	global	110	130	144	96
		weighted	2.08	4.91	1.70	8.57
	H_2O	global	176	229	219	163
D. desulfuricans ATCC 27774	$SO_2^{\bullet-}$	global	103	103	179	92
		weighted	1.93	3.54	3.25	8.91
	H_2O	global	180	199	235	143
D. africanus	$SO_2^{\bullet-}$	global	114	225	173	67
		weighted	2.95	5.73	1.80	4.11
	H_2O	global	196	264	222	82
Dsm. norvegicum	$SO_2^{\bullet-}$	global	106	335	167	92
		weighted	2.60	7.62	1.58	4.49
	H_2O	global	152	340	232	138
Dsm. baculatum	$SO_2^{\bullet-}$	global	98	308	169	95
		weighted	2.22	5.88	2.00	4.72
	H_2O	global	148	333	219	128
D. africanus TpIIc_3	$SO_2^{\bullet-}$	global	204	117	117	66
		weighted	6.62	2.54	2.24	2.66
	H_2O	global	244	188	191	91

of a membrane associated cytochrome studied here. The more familiar TpIc_3 all have a lysine patch in the vicinity of haem IV which is implicated in their interaction with hydrogenase whereas the TpIIc_3 receives electrons from TpIc_3 and the lysine patch is absent. The reduction rate of haem III is generally low, but that of haem II is highly variable: haem II in *D. gigas* is virtually unreactive whereas the highest rates found in this study are for haem II in *Dsm. norvegicum* and *Dsm. baculatum*. These observations naturally raise the question of which factors control the reactivity of haems with $SO_2^{\bullet-}$. This is clearly not an effect of driving force, which is treated separately in the models, since the unreactive haem III has the lowest reduction potential in *D. vulgaris* Hildenborough but the highest in *D. africanus* TpIc_3 and *D. desulfuricans* ATCC 27774, and the variable haem II tends to have potentials close to those of haem I, which has consistently intermediate rates.

In view of the exponential dependence of electron transfer rates on distance [55] we consider a distance-weighted accessibility with unit weighting for the haem macrocycle, one tenth for the heavy atoms directly bonded to it, one hundredth for the next atoms, and so on (Table 5).

Haem III is one of the most accessible to solvent in each of these proteins, but this exposure is dominated by the propionate groups which actually block access to the porphyrin. According to the weighted accessibility for the reducing agent haem III becomes one of the least accessible, in accordance with its low reactivity. Conversely, the haems IV have an intermediate rate despite having the smallest solvent accessibility in each case, but their distance-weighted accessibility is among the largest. Haems I and IV also have significant exposure of the sulphur of thioether 3, which has been implicated in electron transfer [56]. The variable rates of the haems II also show a rough correlation with accessibility. However, accessibility does not explain the high rate observed for haem IV of *D. africanus* TpIIc_3, which is the least accessible of all the haems IV. Also, there is no simple relationship with surface charge since this is the only haem IV in the series not surrounded by lysines, which might be expected to attract the negatively charged reducing agent, and yet it is the only case in which haem IV is clearly more reactive than the others. By contrast, haem I of *D. africanus* TpIIc_3 is significantly more accessible than the other haems I and is surrounded by a region of negative charge which might repel the reducing agent and its rate of reduction is close to the average.

The electronic wavefunctions of the haems are highly anisotropic, as shown by the variation in paramagnetic shifts of the methyl substituents [57,58], and this might be expected to influence the electron transfer rate through the degree of electronic coupling with the reductant. There is remarkably little variation for each haem between the cytochromes studied here, which is a consequence of the fact that the conserved haem geometry extends to the orientation of the axial ligands, possibly to control the intramolecular electron transfer rates. Haems I and IV are solvent accessible in the vicinity of methyls 18^1 and 2^1, both of which show relatively large unpaired spin density. The exposure of haem III involves mainly methyl 2^1, with low spin density, and methyl 12^1 with high density. The largest variation is in the haems II, with exposure of methyl 12^1 which has a relatively low spin density in most cases and a high spin density in *D. africanus* TpIIc_3, and yet the rate of reduction of that haem is similar to that of *D. gigas*.

Thus it appears, unsurprisingly, that close approach of the reductant is a significant factor in controlling the electron transfer rates [55], but it is not dominant in these cytochromes c_3. Factors such as electrostatic charge and electronic coupling also have a role, though no clear trend emerges from the examples examined here and it will be necessary to study a wider range of systems. Nevertheless, this work demonstrates that it is feasible to measure individual rates for similar redox centres in multicentre proteins, taking full account of variations in driving force and pH dependence, and provides a framework for future studies.

Acknowledgments

We thank João Carita for the growth of the organisms, Isabel Pacheco for helping in the purification of the protein and Cláudio Soares for helpful discussions. Financial support was provided by contracts POCTI/QUI/47866/2002 with Fundação para a Ciência e Tecnologia and fellowships to C. M. P. (SFRH/BD/6495/2001) and to D.L.T. (SFRH/BCC/15305/2004) by Fundação para a Ciência e Tecnologia.

References

[1] I.B. Coutinho, A.V. Xavier, Tetraheme cytochromes, Methods Enzymol. 243 (1994) 119–140.
[2] R.O. Louro, T. Catarino, J. LeGall, A.V. Xavier, Redox–Bohr effect in electron/proton energy transduction: cytochrome c_3 coupled to hydrogenase works as a 'proton thruster' in *Desulfovibrio vulgaris*, J. Biol. Inorg. Chem. 2 (1997) 488–491.
[3] J.M. Odom, H.D. Peck Jr., Hydrogenase, electron-transfer proteins, and energy coupling in the sulfate-reducing bacteria *Desulfovibrio*, Annu. Rev. Microbiol. 38 (1984) 551–592.
[4] P.M. Matias, C. Frazão, J. Morais, M. Coll, M.A. Carrondo, Structure analysis of cytochrome c_3 from *Desulfovibrio vulgaris* Hildenborough at 1.9 A resolution, J. Mol. Biol. 234 (1993) 680–699.
[5] M. Czjzek, F. Payan, F. Guerlesquin, M. Bruschi, R. Haser, Crystal structure of Cytochrome c_3 from *Desulfovibrio desulfuricans* Norway at 1.7 A resolution, J. Mol. Biol. 243 (1994) 653–667.
[6] P.M. Matias, J. Morais, R. Coelho, M.A. Carrondo, K. Wilson, Z. Dauter, L. Sieker, Cytochrome c_3 from *Desulfovibrio gigas*: crystal structure at 1.8 A resolution and evidence for a specific calcium-binding site, Protein Sci. 5 (1996) 1342–1354.
[7] S. Norager, P. Legrand, L. Pieulle, C. Hatchikian, M. Roth, Crystal structure of the oxidised and reduced acidic cytochrome c_3 from *Desulfovibrio africanus*, J. Mol. Biol. 290 (1999) 881–902.
[8] R.O. Louro, I. Bento, P.M. Matias, T. Catarino, A.M. Baptista, C.M. Soares, M.A. Carrondo, D.L. Turner, A.V. Xavier, Conformational component in the coupled transfer of multiple electrons and protons in a monomeric tetraheme cytochrome. J. Biol. Chem. 276 (2001) 44044–44051.
[9] I.J. Correia, C.M. Paquete, A. Coelho, C.C. Almeida, T. Catarino, R.O. Louro, C. Frazão, L.M. Saraiva, M.A. Carrondo, D.L. Turner, A.V. Xavier, Proton-assisted two-electron transfer in natural variants of tetraheme cytochromes from *Desulfomicrobium* sp. J. Biol. Chem. 279 (2004) 52227–52237.
[10] L. Pieulle, X. Morelli, P. Gallice, E. Lojou, P. Barbier, M. Czjzek, P. Bianco, F. Guerlesquin, E.C. Hatchikian, The type I/type II cytochrome c_3 complex: an electron transfer link in the hydrogen-sulfate reduction pathway, J. Mol. Biol. 354 (2005) 73–90.
[11] A.C. Messias, D.H.W. Kastrau, H.S. Costa, J. LeGall, D.L. Turner,

H. Santos, A.V. Xavier, Solution structure of *Desulfovibrio vulgaris* (Hildenborough) ferrocytochrome c_3: structural basis for functional cooperativity, J. Mol. Biol. 281 (1998) 719–739.
[12] L. Brennan, D.L. Turner, A.C. Messias, M.L. Teodoro, J. LeGall, H. Santos, A.V. Xavier, Structural basis for the network of functional cooperativities in cytochrome c_3 from *Desulfovibrio gigas*: solution structures of the oxidised and reduced states, J. Mol. Biol. 298 (2000) 61–82.
[13] O. Einsle, S. Foerster, K. Mann, G. Fritz, A. Messerschmidt, P.M. Kroneck, Spectroscopic investigation and determination of reactivity and structure of the tetraheme cytochrome c_3 from *Desulfovibrio desulfuricans* Essex 6, Eur. J. Biochem. 268 (2001) 3028–3035.
[14] H. Santos, J.J.G. Moura, I. Moura, J. LeGall, A.V. Xavier, NMR studies of electron transfer mechanisms in a protein with interacting redox centres: *Desulfovibrio gigas* cytochrome c_3, Eur. J. Biochem. 141 (1984) 283–296.
[15] N. Ravi, I. Moura, C. Costa, M. Teixeira, J. LeGall, J.J. Moura, B.H. Huynh, Mossbauer characterization of the tetraheme cytochrome c_3 from *Desulfovibrio baculatus* (DSM 1743). Spectral deconvolution of the heme components, Eur. J. Biochem. 204 (1992) 779–782.
[16] J.P. Gayda, H. Benosman, P. Bertrand, C. More, M. Asso, EPR determination of interaction redox potentials in a multiheme cytochrome: cytochrome c_3 from *Desulfovibrio desulfuricans* Norway, Eur. J. Biochem. 177 (1988) 199–206.
[17] H. Benosman, M. Asso, P. Bertrand, T. Yagi, J.P. Gayda, EPR study of the redox interactions in cytochrome c_3 from *Desulfovibrio vulgaris* Miyazaki, Eur. J. Biochem. 182 (1989) 51–55.
[18] B. Guigliarelli, P. Bertrand, C. More, R. Haser, J.P. Gayda, Single-crystal electron paramagnetic resonance study of cytochrome c_3 from *Desulfovibrio desulfuricans* Norway Strain. Assignment of the heme midpoint redox potentials, J. Mol. Biol. 216 (1990) 161–166.
[19] P. Bertrand, M. Asso, O. Mbarki, P. Camensuli, C. More, B. Guigliarelli, Individual redox characteristics and kinetic properties of the hemes in cytochromes c_3: new methods of investigation, Biochimie 76 (1994) 524–536.
[20] S.L. Pealing, M.R. Cheesman, G.A. Reid, A.J. Thomson, F.B. Ward, S.K. Chapman, Spectroscopic and kinetic studies of the tetraheme flavocytochrome *c* from *Shewanella putrefaciens* NCIMB400, Biochemistry 34 (1995) 6153–6458.
[21] E.C. Hatchikian, P. Papavassiliou, P. Bianco, J. Haladjian, Characterization of cytochrome c_3 from the thermophilic sulfate reducer *Thermodesulfobacterium commune*, J. Bacteriol. 159 (1984) 1040–1046.
[22] C. Moreno, A. Campos, M. Teixeira, J. LeGall, M.I. Montenegro, I. Moura, C. van Dijk, J.G. Moura, Simulation of the electrochemical behavior of multi-redox systems. Current potential studies on multiheme cytochromes, Eur. J. Biochem. 202 (1991) 385–393.
[23] J.W. Van Leeuwen, C. Van Dijk, H.J. Grande, C. Veeger, A pulse-radiolysis study of cytochrome c_3. Kinetics of the reduction of cytochrome c_3 by methyl viologen radicals and the characterisation of the redox properties of cytochrome c_3 from *Desulfovibrio vulgaris* (Hildenborough), Eur. J. Biochem. 127 (1982) 631–637.
[24] L. Rivas, C.M. Soares, A.M. Baptista, J. Simaan, R.E. Di Paolo, D.H. Murgida, P. Hildebrandt, Electric-field-induced redox potential shifts of tetraheme cytochromes c_3 immobilized on self-assembled monolayers: surface-enhanced resonance Raman spectroscopy and simulation studies, Biophys. J. 88 (2005) 4188–4199.
[25] C.M. Dobson, N.J. Hoyle, C.F. Geraldes, P.E. Wright, R.J.P. Williams, M. Bruschi, J. LeGall, Outline structure of cytochrome c_3 and consideration of its properties, Nature 249 (1974) 425–429.
[26] C.C. McDonald, W.D. Phillips, J. LeGall, Proton magnetic resonance studies of *Desulfovibrio* cytochromes c_3, Biochemistry 13 (1974) 1952–1959.
[27] J.J. Moura, H. Santos, I. Moura, J. LeGall, G.R. Moore, R.J. Williams, A.V. Xavier, NMR redox studies of *Desulfovibrio vulgaris* cytochrome c_3. Electron transfer mechanisms, Eur. J. Biochem. 127 (1982) 151–155.
[28] M. Coletta, T. Catarino, J. LeGall, A.V. Xavier, A thermodynamic model for the cooperative functional properties of the tetraheme cytochrome c_3 from *Desulfovibrio gigas*, Eur. J. Biochem. 202 (1991) 1101–1106.
[29] D.L. Turner, C.A. Salgueiro, T. Catarino, J. LeGall, A.V. Xavier, NMR studies of cooperativity in the tetrahaem cytochrome c_3 from *Desulfovibrio vulgaris*, Eur. J. Biochem. 241 (1996) 723–731.
[30] R.O. Louro, T. Catarino, D.L. Turner, M.A. Piçarra-Pereira, I. Pacheco, J. LeGall, A.V. Xavier, Functional and mechanistic studies of cytochrome c_3 from *Desulfovibrio gigas*: thermodynamics of a "proton thruster", Biochemistry 37 (1998) 15808–15815.
[31] R.O. Louro, T. Catarino, J. LeGall, A.V. Xavier, Cooperativity between electrons and protons in a monomeric cytochrome c_3: the importance of mechano-chemical coupling for energy transduction, ChemBioChem 2 (2001) 831–837.
[32] C.M. Paquete, M.P. Pereira, T. Catarino, D.L. Turner, R.O. Louro, A.V. Xavier, Functional properties of Type I and Type II cytochromes c_3 from *Desulfovibrio africanus*, Biochim. Biophys. Acta, Bioenerg. 1767 (2007) 178–188.
[33] I.J. Correia, C.M. Paquete, R.O. Louro, T. Catarino, D.L. Turner, A.V. Xavier, Thermodynamic and kinetic characterization of trihaem cytochrome c_3 from *Desulfuromonas acetoxidans*, Eur. J. Biochem. 269 (2002) 5722–5730.
[34] V. Favaudon, C. Ferradini, J. Pucheault, L. Gilles, J. LeGall, Kinetics of reduction of the cytochrome c_3 from *Desulfovibrio vulgaris*, Biochem. Biophys. Res. Commun. 84 (1978) 435–440.
[35] I. Tabushi, T. Nishiya, T. Yagi, H. Inokuchi, Kinetic study on the successive four-step reduction of cyt c_3, J. Biochem. 94 (1983) 1375–1385.
[36] T. Yagi, Spectral and kinetic abnormality during the reduction of cytochrome c_3 catalyzed by hydrogenase with hydrogen, Biochim. Biophys. Acta 767 (1984) 288–294.
[37] C. Capeillère-Blandin, F. Guerlesquin, M. Bruschi, Rapid kinetic studies of the electron-exchange reaction between cytochrome c_3 and ferredoxin from *Desulfovibrio desulfuricans* Norway strain and their individual reactions with dithionite, Biochim. Biophys. Acta 848 (1986) 279–293.
[38] J. Haladjian, P. Bianco, F. Guerlesquin, M. Bruschi, Electrochemical study of the electron exchange between cytochrome c_3 and hydrogenase from *Desulfovibrio desulfuricans* Norway, Biochem. Biophys. Res. Commun. 147 (1987) 1289–1294.
[39] T. Catarino, M. Coletta, J. LeGall, A.V. Xavier, Kinetic study of the reduction mechanism for *Desulfovibrio gigas* cytochrome c_3, Eur. J. Biochem. 202 (1991) 1107–1113.
[40] H. Akutsu, J.H. Hazzard, R.G. Bartsh, M.A. Cusanovich, Reduction kinetics of the four haems of cytochrome c_3 from *Desulfovibrio vulgaris* by flash photolysis, Biochim. Biophys. Acta 1140 (1992) 144–156.
[41] T. Catarino, D.L. Turner, Thermodynamic control of electron transfer rates in multicentre redox proteins, ChemBioChem 2 (2001) 416–424.
[42] K. Ozawa, Y. Takayama, F. Yasukawa, T. Ohmura, M.A. Cusanovich, Y. Tomimoto, H. Ogata, Y. Higuchi, H. Akutsu, Role of the aromatic ring of Tyr43 in tetraheme cytochrome c_3 from *Desulfovibrio vulgaris* Miyazaki F, Biophys. J. 85 (2003) 3367–3374.
[43] R.A. Marcus, N. Sutin, Electron transfers in chemistry and biology, Biochim. Biophys. Acta 811 (1985) 265–322.
[44] D.L. Turner, C.A. Salgueiro, J. LeGall, A.V. Xavier, Structural studies of *Desulfovibrio vulgaris* ferrocytochrome c_3 by two-dimensional NMR, Eur. J. Biochem. 210 (1992) 931–936.
[45] P.L. Dutton, Redox potentiometry: determination of midpoint potentials of oxidation–reduction components of biological electron-transfer systems, Methods Enzymol. 54 (1978) 411–435.
[46] C.E. McKenna, W.G. Gutheil, W. Song, A method for preparing analytically pure sodium dithionite. Dithionite quality and observed nitrogenase-specific activities, Biochim. Biophys. Acta 1075 (1991) 109–117.
[47] M. Dixon, The acceptor specificity of flavins and flavoproteins: I. Techniques for anaerobic spectrophotometry, Biochim. Biophys. Acta 226 (1971) 241–258.
[48] D.O. Lambeth, G. Palmer, The kinetics and mechanism of reduction of electron transfer proteins and other compounds of biological interest by dithionite, J. Biol. Chem. 248 (1973) 6095–6103.
[49] C.A. Salgueiro, D.L. Turner, A.V. Xavier, Use of paramagnetic NMR

probes for structural analysis in cytochrome c_3 from *Desulfovibrio vulgaris*, Eur. J. Biochem. 244 (1997) 721–734.

[50] P. Neta, R.E. Huie, A. Harriman, One-electron-transfer reactions of the couple SO_2/SO_2^- in aqueous-solutions—Pulse radiolytic and cyclic voltammetric studies, J. Phys. Chem. 91 (1987) 1606–1611.

[51] H.E.M. Christiansen, I. Coutinho, L.S. Conrad, J.M. Hammerstad-Pedersen, G. Iversen, M.H. Jensen, J.J. Karlsson, J. Ulstrup, A.V. Xavier, Electron transport networks in multicentre metalloproteins, J. Photochem. Photobiol. 82 (1994) 103–115.

[52] G.P. Moss, Nomenclature of tetrapyrroles. Recommendations 1986. IUPAC-IUB Joint Commission on Biochemical Nomenclature (JCBN), Eur. J. Biochem. 178 (1988) 277–328.

[53] P.J. Martel, C.M. Soares, A.M. Baptista, M. Fuxreiter, G. Naray-Szabo, R.O. Louro, M.A. Carrondo, Comparative redox and pKa calculations on cytochrome c_3 from several *Desulfovibrio* species using continuum electrostatic methods, J. Biol. Inorg. Chem. 4 (1999) 73–86.

[54] E. Harada, Y. Fukuoka, T. Ohmura, A. Fukunishi, G. Kawai, T. Fujiwara, H. Akutsu, Redox-coupled conformational alternations in cytochrome c_3 from *D. vulgaris* Miyazaki F on the basis of its reduced solution structure, J. Mol. Biol. 319 (2002) 767–778.

[55] C.C. Page, C.C. Moser, X. Chen, P.L. Dutton, Natural engineering principles of electron tunnelling in biological oxidation–reduction, Nature 402 (1999) 47–52.

[56] G. Tollin, L.K. Hanson, M. Caffrey, T.E. Meyer, M.A. Cusanovich, Redox pathways in electron-transfer proteins: correlations between reactivities, solvent exposure, and unpaired-spin-density distributions, Proc. Natl. Acad. Sci. U. S. A. 83 (1986) 3693–3697.

[57] R.G. Shulman, S.H. Glarum, M. Karplus, Electronic structure of cyanide complexes of hemes and heme proteins, J. Mol. Biol. 57 (1971) 93–115.

[58] D.L. Turner, C.A. Salgueiro, P. Schenkels, J. LeGall, A.V. Xavier, Carbon-13 NMR studies of the influence of axial ligand orientation on haem electronic structure, Biochim. Biophys. Acta 1246 (1995) 24–28.